AMERICAN SOCIETY FOR MICROBIOLOGY | Journal of Virology®

VIRUS-CELL INTERACTIONS

Engineered Oncolytic Poliovirus PVSRIPO Subverts MDA5-Dependent Innate Immune Responses in Cancer Cells

Ross W. Walton,[a] Michael C. Brown,[b] Matthew T. Sacco,[a] Matthias Gromeier[a,b]

[a]Department of Molecular Genetics and Microbiology, Duke University School of Medicine, Durham, North Carolina, USA

[b]Department of Neurosurgery, Duke University School of Medicine, Durham, North Carolina, USA

ABSTRACT We are pursuing cancer immunotherapy with a neuro-attenuated recombinant poliovirus, PVSRIPO. PVSRIPO is the live attenuated type 1 (Sabin) poliovirus vaccine carrying a heterologous internal ribosomal entry site (IRES) of human rhinovirus type 2 (HRV2). Intratumoral infusion of PVSRIPO is showing promise in the therapy of recurrent WHO grade IV malignant glioma (glioblastoma), a notoriously treatment-refractory cancer with dismal prognosis. PVSRIPO exhibits profound cytotoxicity in infected neoplastic cells expressing the poliovirus receptor CD155. In addition, it elicits intriguing persistent translation and replication, giving rise to sustained type I interferon (IFN)-dominant proinflammatory stimulation of antigen-presenting cells. A key determinant of the inflammatory footprint generated by neoplastic cell infection and its role in shaping the adaptive response after PVSRIPO tumor infection is the virus's inherent relationship to the host's innate antiviral response. In this report, we define subversion of innate host immunity by PVSRIPO, enabling productive viral translation and cytopathogenicity with extremely low multiplicities of infection in the presence of an active innate antiviral IFN response.

IMPORTANCE Engaging innate antiviral responses is considered key for instigating tumor-antigen-specific antitumor immunity with cancer immunotherapy approaches. However, they are a double-edged sword for attempts to enlist viruses in such approaches. In addition to their role in the transition from innate to adaptive immunity, innate antiviral IFN responses may intercept the viral life cycle in cancerous cells, prevent viral cytopathogenicity, and restrict viral spread. This has been shown to reduce overall antitumor efficacy of several proposed oncolytic virus prototypes, presumably by limiting direct cell killing and the ensuing inflammatory profile within the infected tumor. In this report, we outline how an unusual recalcitrance of polioviruses toward innate antiviral responses permits viral cytotoxicity and propagation in neoplastic cells, combined with engaging active innate antiviral IFN responses.

KEYWORDS cancer, immunotherapy, innate immunity, MDA5, oncolytic virus, poliovirus, type I interferon, encephalomyocarditis virus

In a 61-patient phase I clinical trial in glioblastoma, intratumoral infusion of PVSRIPO yielded a high incidence of long-term survivors at 36 months after virus infusion, with the first patients alive >6 years post-PVSRIPO (1). Clinical use of PVSRIPO is possible due to profound neuro-attenuation mediated by the foreign human rhinovirus type 2 (HRV2) internal ribosomal entry site (IRES) (2, 3), which forms a ribonucleoprotein complex specifically in neurons that is incompatible with ribosome recruitment (4, 5). PVSRIPO has virtually universal tropism for solid neoplasia cells due to widespread expression of its receptor CD155 (3) on such cells (6, 7). High-titer intracerebral inoculation of PVSRIPO does not cause poliomyelitis or encephalomyelitis in nonhuman

Received 21 May 2018 **Accepted** 6 July 2018

Accepted manuscript posted online 11 July 2018

Citation Walton RW, Brown MC, Sacco MT, Gromeier M. 2018. Engineered oncolytic poliovirus PVSRIPO subverts MDA5-dependent innate immune responses in cancer cells. J Virol 92:e00879-18. https://doi.org/10.1128/JVI.00879-18.

Editor Julie K. Pfeiffer, University of Texas Southwestern Medical Center

Address correspondence to Matthias Gromeier, grome001@mc.duke.edu.

primates (8) or humans (1). Yet unhinged Raf-ERK1/2-MNK1/2 signaling in neoplasia provides an advantage to viral IRES-mediated translation; thus, PVSRIPO retains translation competence, proliferation capacity, and cytotoxicity in neoplastic cells (9–11).

Innate antiviral responses to infection of neoplastic cells and components of the tumor microenvironment likely play a pivotal role in shaping PVSRIPO immunotherapy. These responses may also determine the character of the compound immunogenic signal emanating from infected/damaged tumor cells and its ability to instigate adaptive antitumor immunity (12). However, there is compelling evidence that intact type I interferon (IFN) responses mounted by infected cancer cells prevents *in vitro* oncolysis and overall antitumor efficacy of various oncolytic virus platforms (i.e., vesicular stomatitis virus, oncolytic herpes simplex virus 1, Semliki Forest virus, or measles vaccine virus) (13–16). A relative insensitivity to type I IFN signaling of wild-type poliovirus (PV) has been reported (17). Thus, given PVSRIPO's promise in the clinic, we sought to decipher the relation of PVSRIPO to host innate IFN responses in neoplastic cells.

Melanoma differentiation-associated protein 5 (MDA5), a cytoplasmic pattern recognition receptor (PRR) that recognizes long, double-stranded RNA (dsRNA) of picornavirus replicative intermediates (18), is the main inducer of type I IFN in response to picornaviruses (19). Once activated, MDA5 filaments translocate to mitochondria and bind to mitochondrial antiviral signaling protein (MAVS), leading to IRF3 phosphorylation by tank-binding kinase 1 (TBK1) and IκB kinase ε (IKKε) (20) and type I IFN induction (21). Secreted type I IFNs bind to IFN-α/β receptor (IFNAR) and activate the signal transducer and activator of transcription 1 (STAT1). Active STAT1 serves as part of a transcription factor complex that upregulates IFN-stimulated genes (ISGs), e.g., OAS1, MDA5, IFIT1, and STAT1 (22).

Here, we show subversion of innate antiviral signals by PVSRIPO in melanoma and glioma cells. PVSRIPO was refractory to endogenous innate responses upstream of IFN initiated by MDA5 during infection or activation of Toll-like receptor 3 (TLR3) with poly(I·C) prior to infection and downstream of IFN following pretreatment of cells with IFN-α. Although engaging PRRs dampened PVSRIPO dynamics, PVSRIPO achieved cytopathogenic viral translation and propagation in cells with ongoing active IFN responses. This effect did not involve active viral interference with response modifiers in the IFN induction pathway; rather, our investigations suggest that PVSRIPO's translation strategy, combined with drastic effects on host cell integrity, preclude antiviral immune suppression of viral replication, allowing PVSRIPO to evade innate antiviral responses.

RESULTS

PVSRIPO translation, propagation, and cytotoxicity are not intercepted by intrinsic type I IFN responses in melanoma cells. In contrast to emblematic positive-strand (encephalomyocarditis virus [EMCV]) or negative-strand (vesicular stomatitis virus) RNA viruses, pretreatment of HeLa cells with IFN-α does not preclude wild-type PV1 (Mahoney) propagation in HeLa cells (17). To assess the interaction of PVSRIPO and the innate antiviral IFN response in a more relevant context, we infected a panel of human melanoma cell lines and assayed innate immune signals and viral translation, propagation, and cytotoxicity over time (Fig. 1). We chose melanoma cell lines for several reasons: (i) CD155 expression is widespread on melanoma cells in patients (23, 24); (ii) PVSRIPO is currently being developed for clinical investigations in this indication; (iii) important mechanistic information on how PVSRIPO engages tumor-associated antigen-specific antitumor immunity *in vivo* was obtained in the classic B16 immunocompetent mouse melanoma model (12).

To avoid bias due to this variable, the three melanoma cell lines in our panel, DM440, -443, and -6, were all positive for the BRAF (V600E) mutation commonly associated with melanoma (25). These cells were uniformly susceptible to PVSRIPO infection (Fig. 1A). DM440 and DM6 responded to PVSRIPO infection with STAT1 (Y701) phosphorylation (Fig. 1A and B) and IFN-β release (Fig. 1D), indicating an intact antiviral type I IFN response. PVSRIPO-infected DM443 cells did not induce phospho (p)-STAT1

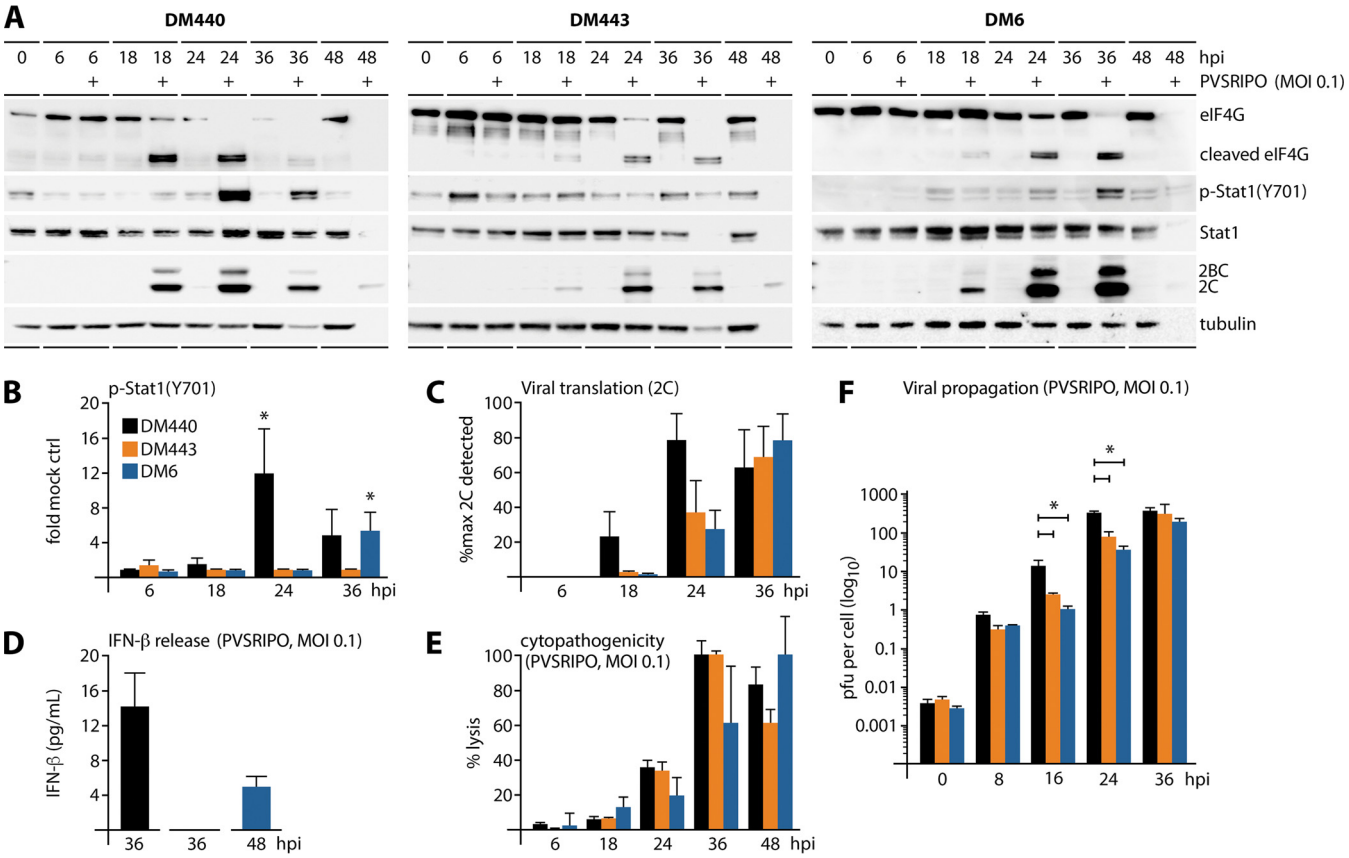

FIG 1 Melanoma cell-intrinsic type I IFN responses do not affect PVSRIPO translation, growth, or cytotoxicity. Melanoma cell lines (DM440, -443, and -6) were mock or PVSRIPO infected at an MOI of 0.1. (A) Lysates, collected at the indicated time postinfection, were analyzed by immunoblotting for viral translation (2BC/2C), cytotoxicity (eIF4G cleavage), and type I IFN response [p-STAT1 (Y701)]; blots are representative of at least four independent series. (B) Fold change in p-STAT1 (Y701) relative to that in mock-infected controls ($n = 4$; *, $P < 0.05$). (C) Viral 2C as percentage of maximum detected 2C ($n = 4$). (D) IFN-β release from PVSRIPO-infected melanoma cells as determined by ELISA ($n = 4$). (E) Percent cytotoxicity by LDH release from infected cells ($n = 4$). (F) Multistep growth curves of PVSRIPO in melanoma cells ($n = 3$; *, $P < 0.05$, for results with DM440 versus those with DM443 and DM6 cells at 16 and 24 hpi). For all panels, values are means ± SEM.

(Y701) (Fig. 1A and B) or release of IFN-β (Fig. 1D). Viral translation varied between melanoma cell types, but DM440 cells consistently showed higher expression of viral proteins than the other cell lines (Fig. 1C). We determined that DM443 cells respond to exogenous IFN-α in the same manner as DM440 and DM6 (data not shown), indicating that these cells harbor deficits in sensing viral RNA, in transmitting signal to IRF3, or in type I IFN biosynthesis.

The kinetics of viral translation and cytotoxicity (eukaryotic initiation factor 4G1 [eIF4G1; referred to as eIF4G] cleavage [26]) did not vary significantly in the three melanoma cell lines (Fig. 1A). In fact, DM440, which had the strongest IFN-β release/p-STAT1 (Y701) phenotype (Fig. 1B and D), was most permissive for viral translation/cytopathogenicity (Fig. 1A, C, and E). Lytic cell death after PVSRIPO infection was quantified by measuring lactose dehydrogenase (LDH) release; 100% cell killing by 36 h postinfection (hpi) (DM440, DM443) or 48 hpi (DM6) (Fig. 1E) closely agreed with immunoblotting results. Host cell lysis in samples with maximal viral propagation yields was invariably associated with global loss of sample protein, including the tubulin loading controls (Fig. 1A).

We deliberately used multiplicities of infection (MOIs) of $\leq$0.1 throughout this study to capture the effect of innate antiviral responses on multiple successive virus propagation rounds. Since host cell entry of PV RNA is inherently inefficient, due to CD155-mediated particle disintegration (27) and sloughing off of noninfectious virus particles (27, 28), the actual MOI is lower than the intended MOI. Indeed, after a 60-min

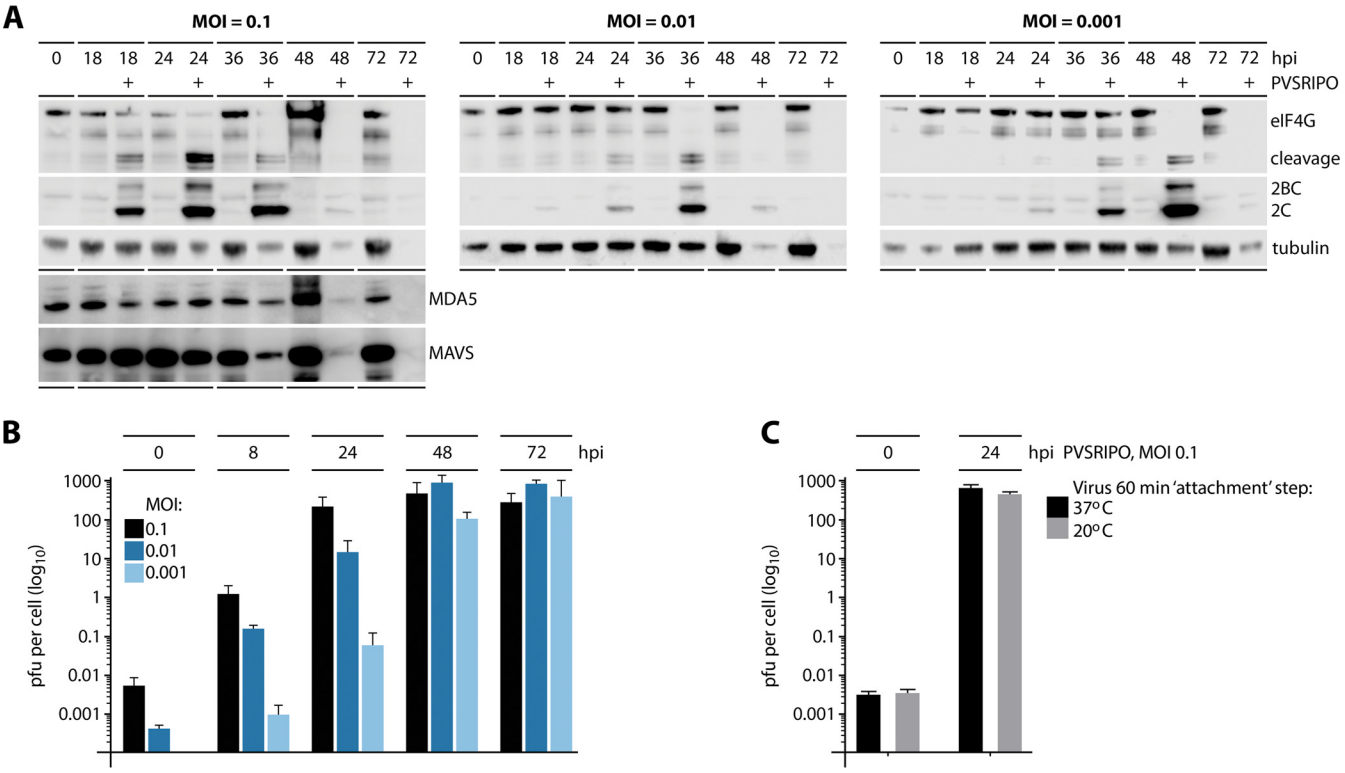

FIG 2 PVSRIPO propagation and cytotoxicity occur at extremely low MOIs in IFN-competent melanoma cells and does not involve viral interference with MDA5 or MAVS. DM440 cells were mock/PVSRIPO-infected at MOIs of 0.1, 0.01, and 0.001. (A) Cell lysates collected at the indicated time postinfection were analyzed by immunoblotting for viral translation (2BC/2C), cytotoxicity (eIF4G cleavage), and innate immune proteins (MDA5 and MAVS); blots are representative of two independent series. (B) Multistep growth curves of PVSRIPO at an MOI of 0.1, 0.01, and 0.001. Values are means ± SEM ($n = 3$). (C) Multistep growth curve of DM440 cells infected with PVSRIPO at an MOI of 0.1 and a 1-h attachment step at 37°C or 20°C (means ± SEM; $n = 3$).

attachment step, we recovered only ~0.004 PFU per cell in DM440/443/6 cells infected with PVSRIPO at an MOI of 0.1 (Fig. 1F and 2). Thus, our assay with initial infection of <1% of host cells in the culture was suitable to interrogate the effect of the innate antiviral IFN response on the dynamics of multiple rounds of PVSRIPO replication *in vitro*. PVSRIPO propagation was logarithmic in all three melanoma cell lines, with DM440 exhibiting the most prolific growth (Fig. 1F). These results indicate that PVSRIPO exhibits full cytopathogenic and replication potential in melanoma cells at low MOIs, regardless of the presence of an active type I IFN response.

PVSRIPO replicates in and kills IFN-competent melanoma cells at extremely low MOIs without specific cleavage of MDA5 or its downstream effector MAVS. Many viral pathogens must intercept antiviral IFN responses to replicate in the face of activating innate immunity (29). It has been claimed that enteroviruses actively prevent type I IFN responses through proteolytic cleavage of MDA5, MAVS, or other innate antiviral response modifiers as viral strategies of innate immune evasion. The published record is contradictory on the mechanism of these purported proteolytic cleavages. Putative MDA5 cleavage in enterovirus-infected cells was reported either to rely on the viral 2A protease ($2A^{pro}$) (30) or, independent of $2A^{pro}$, to occur in a proteasome/caspase-dependent manner (31). Presumptive cleavage of MAVS was specifically linked to either $2A^{pro}$ (30) or viral $3C^{pro}$ (32).

We examined the possibility of a role for the purported MDA5 or MAVS cleavage in IFN subversion by PVSRIPO (Fig. 2A). IFN-competent DM440 cells were infected with PVSRIPO at an MOI of 0.1 (as described in the legend of Fig. 1A); viral translation and eIF4G cleavage (by $2A^{pro}$) were juxtaposed to MDA5 and MAVS in immunoblots (Fig. 2A, left). In step with productive viral translation, eIF4G cleavage was prominent by 18 hpi. We did not observe concomitant changes to MDA5/MAVS abundance or integrity

at these intervals (Fig. 2A). Both MDA5 and MAVS levels declined at 36 to 72 hpi. However, this occurred in parallel to the characteristic loss of immunoblot signal (e.g., loss of tubulin loading control) that is invariably observed in samples with rampant lytic enterovirus cytotoxicity (e.g., at intervals of maximal virus propagation). The absence of MDA5/MAVS degradation in the presence of prominent eIF4G cleavage likely excludes $2A^{pro}$-mediated proteolysis. MDA5/MAVS may be affected by the gross, indiscriminate proteolytic degradation that occurs with enterovirus-induced cell lysis (particularly in cells infected at MOIs of $\geq$10), consistent with observations by Barral et al. (31). However, such degradation in destroyed cells does not constitute a viral mechanism to intercept innate IFN responses; rather, it represents a passive bystander effect of drastic viral cytopathogenicity. Thus, we cannot confirm any of the mutually contradictory versions claiming enterovirus interference with MDA5 or MAVS as a mechanism of innate immune evasion. This is in accordance with our observations of IFN-β release and STAT1 (Y701) phosphorylation in PVSRIPO-infected DM440 and DM6 cells (Fig. 1A).

PVSRIPO IFN subversion is dose (MOI) independent. If PVSRIPO spread is not contained by the antiviral type I IFN response in IFN-competent melanoma cells, viral cytotoxicity and propagation should occur regardless of the MOI. To test this, we infected DM440 cells at three different MOIs (0.1, 0.01, and 0.001) and tracked viral cytopathogenicity and propagation (Fig. 2A and B). As mentioned above, inefficient entry means that the intended MOIs differed from the actual MOIs (Fig. 1F). Tests recovering host cell-associated infectious PVSRIPO after the attachment step revealed actual MOIs of $\sim$0.006 and $\sim$0.0004 for the intended MOIs of 0.1 and 0.01, respectively; we could not recover virus from DM440 cells infected at an MOI of 0.001 (implying an actual MOI of $\sim$0.00004 to 0.00006) (Fig. 2B). Infection of DM440 cells with PVSRIPO revealed significant viral translation and host cytotoxicity at all tested MOIs (Fig. 2A). Lower MOIs simply delayed the kinetics of these events; peak viral translation preceding complete cytolysis was observed at 24 (MOI of 0.1), 36 (MOI of 0.01), or 48 (MOI of 0.001) hpi, respectively (Fig. 2A).

Classically, a 30- to 60-min attachment step at room temperature is performed for poliovirus growth curves to synchronize viral entry (10). We avoided this step in all of our assays because the temperature shift alone induced p-STAT1 (Y701), interfering with our analyses. Therefore, the 60-min attachment step was carried out at 37°C. This could have encouraged virus entry and eclipse at the 0-h interval, thus accounting for the low recovery of virus immediately after the attachment step. To exclude this possibility, we carried out the test with an attachment step at 20°C, which precludes viral entry (33). This test revealed similar PFU recovery at 20° and 37°C after the 60-min attachment step and at 24 hpi, indicating that the attachment step temperature is not a factor in low virus recovery at the 0-h interval (Fig. 2C). Our findings confirm that unimpeded PVSRIPO translation, host cytotoxicity, and proliferation/spread occur in the presence of an active host type I IFN response, do not involve active viral interference with MDA5 or MAVS, and are independent of the input dose, at least at MOIs of $\geq$0.001.

Innate immune responses to PVSRIPO and EMCV are MDA5 dependent and inhibit EMCV to a greater extent than PVSRIPO. To gauge the PVSRIPO-MDA5 relationship in infected melanoma cells and to compare PVSRIPO to a distant relative, EMCV, with IFN sensitivity in human host cells (17), stable MDA5-depleted DM440 and DM6 cells were generated with lentiviral short hairpin RNA (shRNA) transduction (see Materials and Methods). Effective MDA5 depletion in DM440 cells infected with PVSRIPO or EMCV (MOI of 0.1) was evident as nearly complete loss of MDA5 immunoblot signal (Fig. 3A and B) and a loss of IFN-β release in infected, MDA5-depleted DM440 cells (Fig. 3C; only data for PVSRIPO are shown) and almost completely abolished p-STAT1 (Y701) induction (Fig. 3A, B, and D). Loss of p-STAT1 (Y701) and IFN-β release upon MDA5 depletion confirm MDA5's pivotal role in the innate antiviral IFN response to picornaviruses. MDA5 depletion had no significant effect on PVSRIPO translation (P2, 2BC, and 2C viral proteins) or eIF4G cleavage in DM440 cells infected at an MOI of 0.1 (Fig. 3A). There was an increase in viral propagation in MDA5-depleted cells, with viral

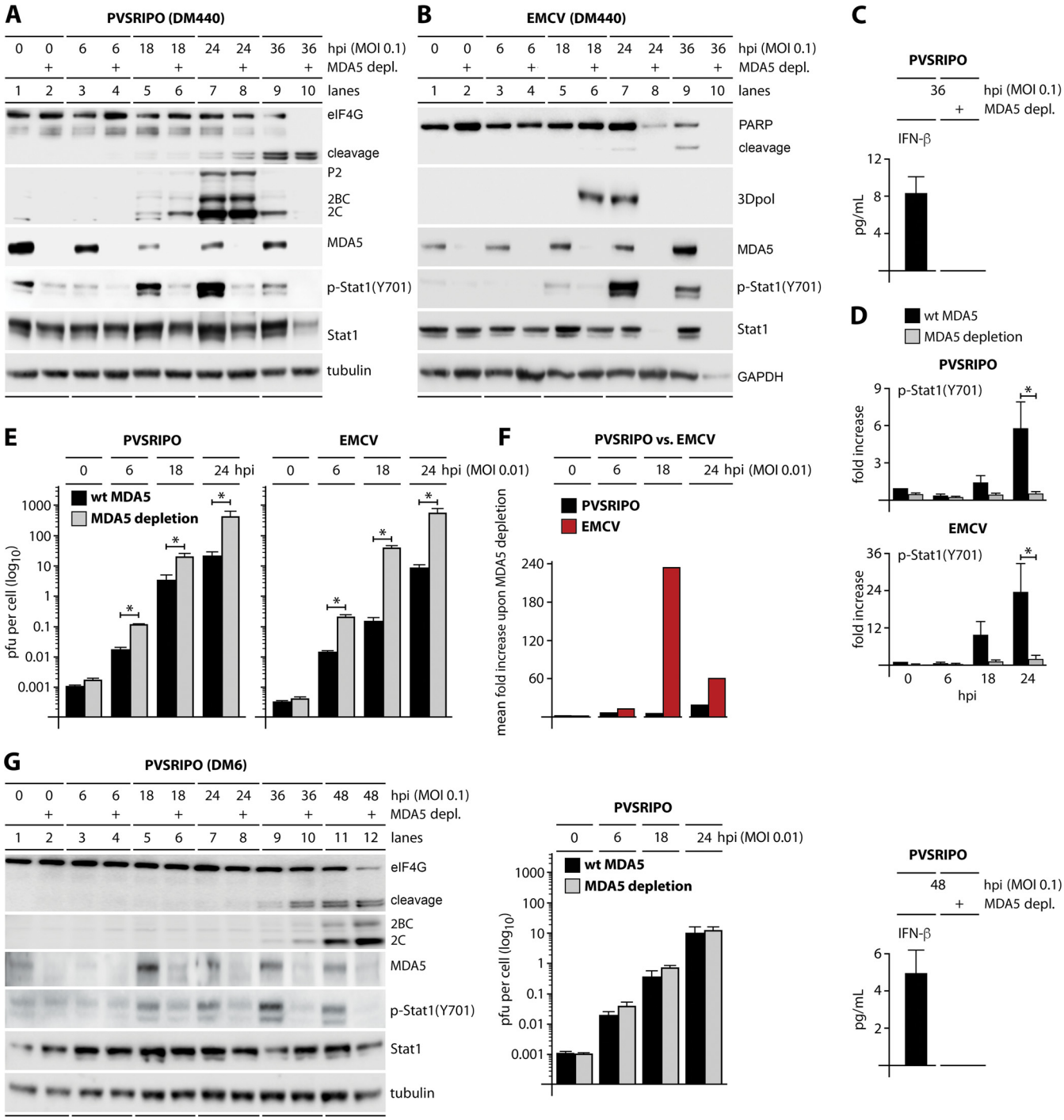

FIG 3 PVSRIPO and EMCV stimulate innate immune responses through MDA5 which suppress replication of EMCV but not PVSRIPO. Parental wild-type (wt) and stably MDA5-depleted DM440 and DM6 cells were mock infected (0 h) or infected with either PVSRIPO (DM440 and DM6) or EMCV (DM440). (A and B) Immunoblots of cell lysates collected at the indicated time postinfection from DM440 cells infected with PVSRIPO (A) or EMCV (B) at an MOI of 0.1 were analyzed for markers of viral cytotoxicity (eIF4G and PARP cleavage), viral translation (2C/2BC for PVSRIPO and $3D^{pol}$ for EMCV), and the innate response [MDA5, p-STAT1 (Y701), and STAT1]; immunoblots are representative of at least four independent experiments. (C) ELISA of IFN-β secreted from wild-type and MDA5-depleted DM440 cells infected with PVSRIPO at an MOI of 0.1 (means $\pm$ SEM; $n = 4$). (D) Fold increase of p-STAT1 (Y701) in PVSRIPO-infected or EMCV-infected DM440 cells relative to levels in mock-infected cells (0 hpi) at an MOI of 0.1 (means $\pm$ SEM; $n = 4$). *, $P < 0.05$, for results with wild-type cells versus those in MDA5-depleted cells (24 hpi). (E) Multistep growth curves of PVSRIPO and EMCV in DM440 wild-type parental and MDA5-depleted cells infected at an MOI of 0.01 (means $\pm$ SEM; $n = 3$). *, $P < 0.05$, for results in wild-type cells versus those in MDA5-depleted cells at 6, 18, and 24 hpi. (F) Fold increase of mean viral titer in wild-type versus MDA5-depleted DM440 cells infected with PVSRIPO or EMCV at an MOI of 0.01. (G) Immunoblots of cell lysates collected at the indicated time postinfection from PVSRIPO-infected DM6 cells at an MOI of 0.1 were analyzed as described for panel A (left). Multistep growth curves of PVSRIPO in DM6 wild-type (wt) parental and MDA5-depleted cells infected at an MOI of 0.01 were performed (means $\pm$ SEM; $n = 3$) (middle). ELISA of IFN-β secreted from wild-type and MDA5-depleted DM6 cells infected with PVSRIPO at an MOI of 0.1 was performed (means $\pm$ SEM; $n = 4$) (right).

titers elevated ~6-fold at 18 hpi (Fig. 3E and F). Similarly, MDA5 depletion abolished IFN-β release from DM6 cells but had no significant effect on PVSRIPO translation and propagation (Fig. 3G).

In sharp contrast, MDA5 depletion in DM440 cells had a profound effect on EMCV. MDA5-depleted cells permitted earlier expression of viral $3D^{pol}$ than the parental line, as well as accelerated lytic cell death as measured by global loss of cellular proteins [e.g., poly(ADP-ribose) polymerase (PARP) and STAT1] (Fig. 3B). EMCV $3D^{pol}$ levels were higher in wild-type than in MDA5-depleted cells at 24 hpi because the infected MDA5-depleted cells were already destroyed at this interval (Fig. 3B). MDA5 depletion elevated EMCV propagation ~240-fold at 18 hpi (Fig. 3E and F). A lack of an effect of MDA5 depletion on PVSRIPO translation and growth resonates with our finding of unimpeded virus spread/propagation at extremely low MOIs in type I IFN-competent cultures (Fig. 2).

PVSRIPO, but not EMCV, subverts type I IFN responses in melanoma cells. To further decipher the virus-host innate immune relationship of PVSRIPO versus EMCV, DM440 melanoma and DU54 glioma cells were pretreated with 100 U/ml recombinant human IFN-α2a or vehicle in growth medium (24 h) and then infected with either PVSRIPO or EMCV (MOIs of 0.1 and 0.01) along with appropriate mock-infected controls (Fig. 4). IFN-α2a pretreatment of DM440 cells increased MDA5 and OAS1 expression (Fig. 4A and B) and p-STAT1 (Y701) (Fig. 4A, B, and C) throughout the assay, indicating sustained ISG expression and IFNAR downstream signaling. IFN-α2a pretreatment inhibited incipient eIF4G cleavage in PVSRIPO-infected DM440 cells starting at 6 hpi and throughout the assay until 36 hpi. However, even in IFN-α2a-pretreated DM440 cells, substantial eIF4G cleavage took place (Fig. 4A). This was mirrored by productive viral translation (Fig. 4A and D) and robust levels of virus propagation in IFN-α2a-pretreated DM440 cells throughout the assay; viral growth was reduced but only ~50-fold at 24 hpi (Fig. 4E).

In contrast, IFN-α2a pretreatment of DM440 cells virtually abolished EMCV translation at any interval (Fig. 4B) and reduced viral propagation >12,000-fold at 24 hpi (Fig. 4E). In fact, while PVSRIPO infection of IFN-α2a-pretreated cells yielded ~10 PFU/cell at 48 hpi, the value was only ~0.01 PFU/cell at 48 hpi with EMCV infection (Fig. 4E). IFN-α2a pretreatment also protected DM440 cells from EMCV cytopathogenicity (Fig. 4B, PARP cleavage).

Similar to pretreatment of DM440 cells, pretreatment of DU54 glioma cells with IFN-α2a induced p-STAT1 (Y701) and expression of ISGs, including STAT1 and IFIT1 (Fig. 4F). Unlike DM440 cells, DU54 cells do not have an intrinsic IFN response to PVSRIPO infection although they respond to exogenous type I IFNs (Fig. 4F). IFN-α2a pretreatment of DU54 cells delayed eIF4G cleavage and 2C translation, but this delay was temporary; and PVSRIPO overcame this inhibition almost completely by 30 hpi (Fig. 4F and G). PVSRIPO propagation was reduced by a maximum of ~10-fold at 6 hpi in IFN-α2a-pretreated DU54 cells (Fig. 4H).

Endogenous PVSRIPO and EMCV propagation is resistant to auto-/paracrine type 1 IFN. We used p-STAT1 (Y701) as a marker for MDA5-dependent type I IFN responses elicited by PVSRIPO or EMCV. Type I and III IFNs cause autocrine and paracrine antiviral immune responses through STAT1 (Y701) phosphorylation (34). However, *in vitro* studies suggested that STAT1 activation may also occur with non-IFN cytokines, e.g., interleukin-6 (IL-6), IL-10, colony-stimulating factor 1 (CSF1), or growth factors, such as epidermal/platelet-derived growth factors (discussed in reference 35). To unambiguously demonstrate that induction of p-STAT1 (Y701) indeed correlates with the antiviral type I IFN response in our experiments, we blocked IFNAR with anti-IFNAR2 antibodies prior to and during virus infection (Fig. 5). DM440 cells were mock treated (no antibody) or pre- and cotreated with isotype-matched control antibody (control) or anti-IFNAR2 antibody (IFNAR), followed by infection by PVSRIPO or EMCV at an MOI of 0.1 (Fig. 5A and B). IFNAR blockade almost completely prevented STAT1 (Y701) phosphorylation induced by PVSRIPO or EMCV infection (Fig. 5A and B).

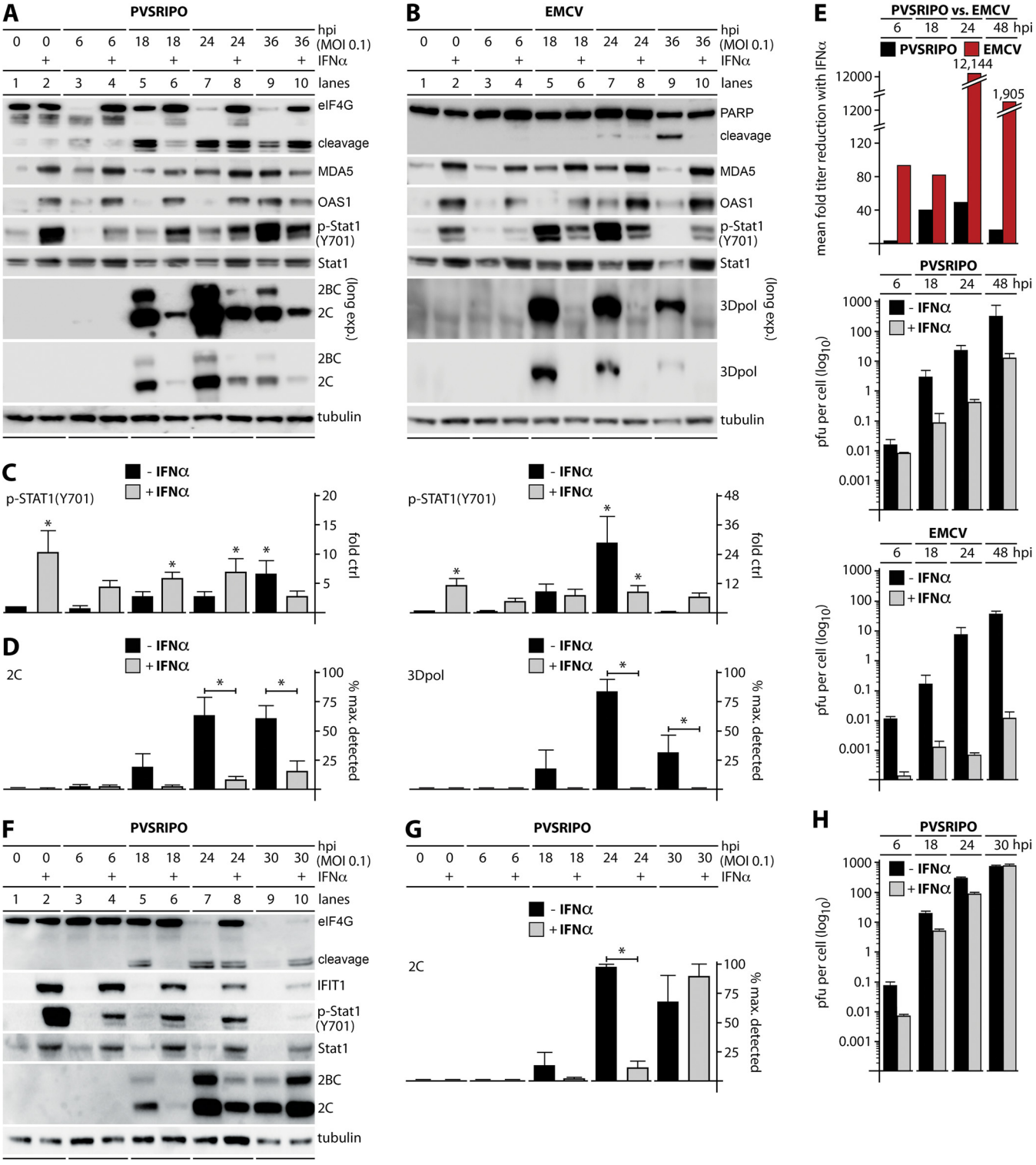

FIG 4 PVSRIPO translation, propagation, and lethal cytopathogenicity occur in IFN-pretreated melanoma and glioma cells. Cells were pretreated with 100 U/ml recombinant human IFN-α2a (+) or vehicle (24 h) prior to mock (0 h), PVSRIPO (DM440 and DU54), or EMCV (DM440) infection. (A and B) Lysates from DM440 cells infected with PVSRIPO or EMCV at an MOI of 0.1 were collected and analyzed by immunoblotting as described in the legend of Fig. 3. Immunoblots are representative of at least five independent experiments. (C) Fold increase in p-STAT1 (Y701) in IFN-α2a- or vehicle-pretreated DM440 cells after PVSRIPO (left column) or EMCV (right column) infection at an MOI of 0.1 (means ± SEM; $n = 5$). *, $P < 0.05$, for results versus those in the mock-treated control. (D) Viral protein expression in IFN-α2a- or vehicle-pretreated DM440 cells after PVSRIPO (2C, left) or EMCV ($3D^{Pol}$, right) infection at an MOI of 0.1 as a percentage of maximum detected viral protein (means ± SEM; $n = 5$). *, $P < 0.05$, for results in IFN-pretreated cells versus those in untreated cells. (E) Fold reduction in mean viral titer (top) and multistep growth curves of PVSRIPO (middle) and EMCV (bottom) were performed in IFN-α2a- or vehicle-pretreated DM440 cells at an MOI of 0.01 (means ± SEM; $n = 3$). (F) Lysates from DU54 cells were collected and analyzed by immunoblotting for markers of viral cytotoxicity (eIF4G cleavage), viral translation (2C/2BC), and the innate antiviral response [IFIT1, (p-STAT1 (Y701), and STAT1]. Immunoblots are representative of two independent

(Continued on next page)

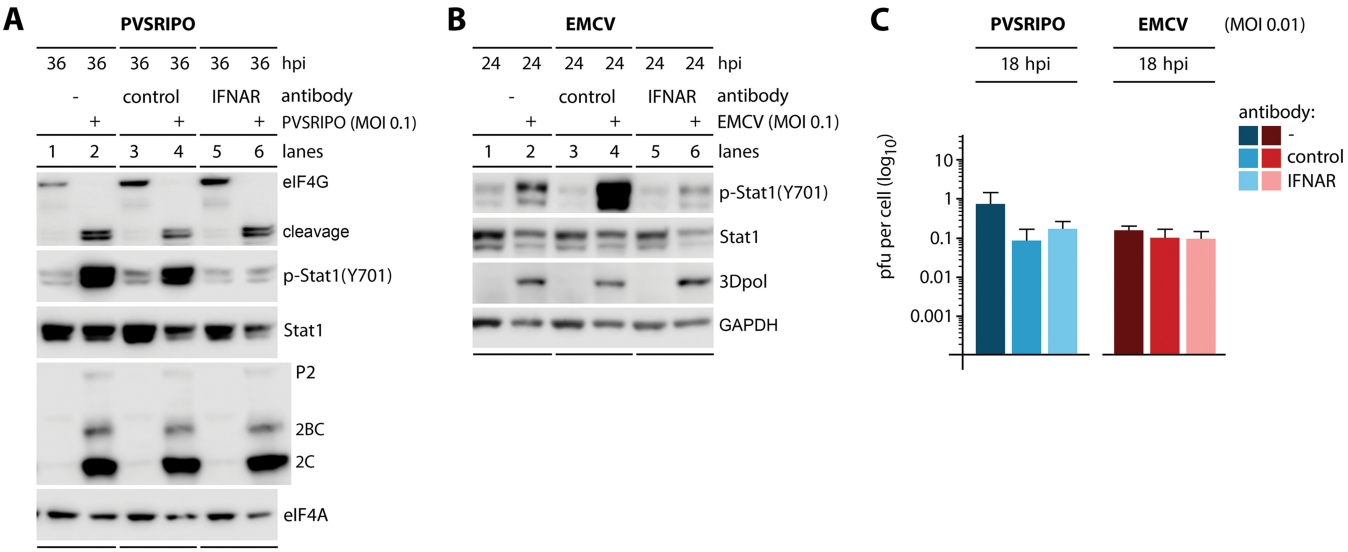

FIG 5 Inhibition of p-STAT1 (Y701) in PVSRIPO or EMCV-infected DM440 cells by IFNAR blockade has no effect on either virus. DM440 cells were mock treated (no antibody; lanes 1 and 2) or pretreated with isotype-matched control antibody (lanes 3 and 4) or 1 μg/ml IFNAR2 blocking antibody (lanes 5 and 6) (24 h) and then cotreated with antibody and mock, PVSRIPO, or EMCV infected. (A and B) Lysates from cells mock and PVSRIPO infected or mock and EMCV infected at an MOI of 0.1 were collected at the indicated time postinfection and analyzed by immunoblotting as described in the legend of Fig. 1. Immunoblots are representative of two independent experiments. (C) Virus yields of PVSRIPO/EMCV-infected DM440 cells (MOI of 0.01) were determined at 18 hpi (means $\pm$ SEM; $n = 3$). No statistically significant differences were found.

Thus, picornavirus-induced p-STAT1 (Y701) *in vitro* is mostly due to type I IFNs. In accordance with observations reported with MDA5 depletion (Fig. 3) and IFN-α2a pretreatment (Fig. 4), intercepting type I IFN signaling had no influence on PVSRIPO translation, eIF4G cleavage (Fig. 5A), or propagation (Fig. 5C).

Surprisingly, IFNAR blockade also had no effect on translation (Fig. 5B) and propagation of EMCV (Fig. 5C). In contrast, MDA5 depletion enhanced EMCV translation substantially (Fig. 3B) and elevated viral propagation (18 hpi) ~240-fold (Fig. 3E and F). Also, IFN-α2a pretreatment almost completely abolished EMCV translation and depressed viral propagation ~12,000-fold (24 hpi). These observations suggest (i) that the host innate antiviral immune response intercepts EMCV in infected cells downstream of MDA5 engagement and upstream of type I IFN release and (ii) that PVSRIPO subverts innate antiviral defenses by interfering with or evading this stage of the type I IFN response.

EMCV is susceptible to endogenous innate antiviral responses upstream of IFN release. We considered two scenarios that could explain differential effects of MDA5 activation on PVSRIPO versus EMCV in infected host cells: (i) MDA5 may exert antiviral effects directly, e.g., by associating with viral dsRNA and disrupting viral protein-dsRNA ribonucleoprotein assemblies (36); (ii) intrinsic antiviral transcriptional programs, e.g., via IRF3 and NF-κB, could intercept the viral life cycle endogenously. Either scenario could play out differently in PVSRIPO- and EMCV-infected cells. First, we compared the effect of the small-molecule kinase inhibitor BX795, a relatively specific inhibitor of TBK1 and IKKε (37), on PVSRIPO and EMCV. Pretreatment of DM440 cells with BX795 abolished p-STAT1 (Y701) in infected cells (Fig. 6A and B) and roughly mimicked the effects of MDA5 depletion on PVSRIPO and EMCV translation (Fig. 6A and B; compare 3A and B). At peak viral translation (24 hpi), PVSRIPO protein synthesis was enhanced ~1.8-fold (Fig. 6A). In contrast, peak EMCV translation (18 hpi) was substantially elevated in a statistically significant manner (~40-fold) (Fig. 6B). As with MDA5 deple-

FIG 4 Legend (Continued)
experiments. (G) Viral protein expression in IFN-α2a- or vehicle-pretreated DU54 cells after PVSRIPO infection at an MOI of 0.1 as a percentage of maximum detected viral protein (means $\pm$ SEM; $n = 2$). *, $P < 0.05$, for results in IFN-pretreated cells versus those in untreated cells (24 hpi). (H) Multistep growth curves of PVSRIPO in IFN-α2a- or vehicle-pretreated DU54 cells at an MOI of 0.01 (means $\pm$ SEM; $n = 3$).

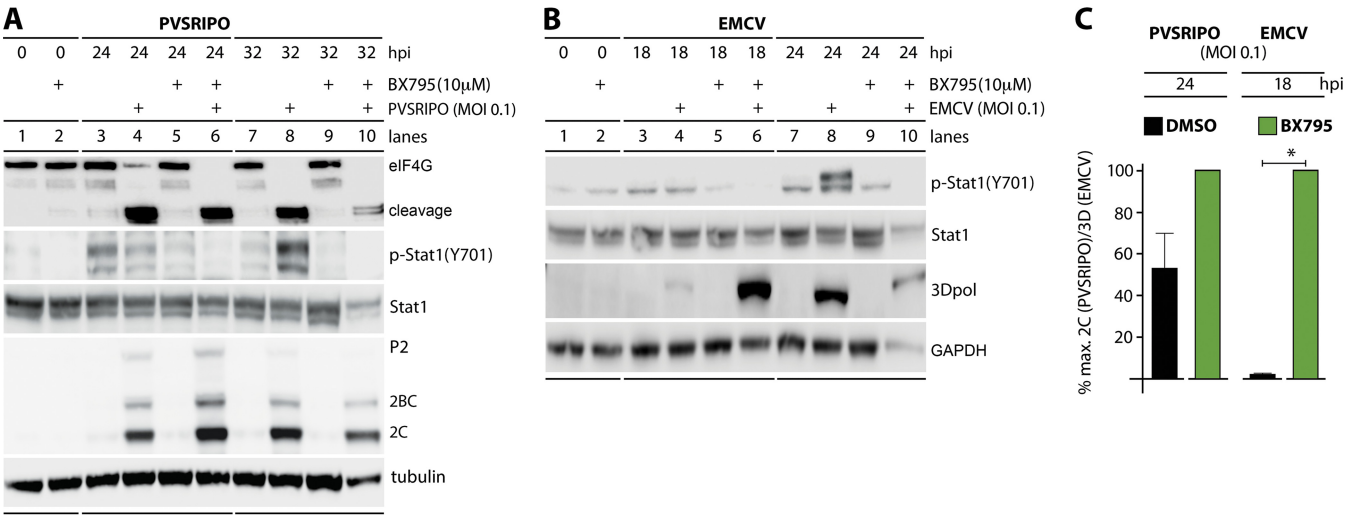

FIG 6 TBK1/IKKε inhibition promotes EMCV translation with little effect on PVSRIPO translation in infected DM440 cells. DM440 cells were pretreated with 10 μM BX795 (1 h) or a DMSO control and then mock infected or infected with virus at an MOI of 0.1. (A and B) Lysates were collected at the indicated time postinfection from control cells, and cells were infected with PVSRIPO or EMCV and analyzed by immunoblotting as described in the legend of Fig. 1. Immunoblots are representative of two independent experiments. (C) Viral protein expression in BX795- or DMSO-pretreated DM440 cells after PVSRIPO (2C) or EMCV ($3D^{pol}$) infection at an MOI of 0.1 (24 and 18 hpi, respectively) as a percentage of maximum detected viral protein (means $\pm$ SEM; $n = 2$). *, $P < 0.05$, for results with BX795 treatment versus those in the mock-treated control.

tion, EMCV-infected cells pretreated with BX795 were killed/lysed by 24 hpi, which is why viral translation was higher in mock pretreated cells at this interval (Fig. 6B).

Our observations suggest that EMCV is susceptible to innate immune events elicited by MDA5 (hence, its substantial benefit upon MDA5 depletion) (Fig. 3B) and the transcriptional programs activated by downstream TBK1/IKKε (Fig. 6B). Since BX795 and MDA5 depletion produced similar patterns of enhanced EMCV translation, direct effects of MDA5 on EMCV are unlikely to play a significant role in the innate antiviral host response. To conclusively exclude direct effects of MDA5 on PVSRIPO/EMCV as a factor in the differential innate antiviral host response to these agents, we carried out experiments in MDA5-depleted DM440 cells combined with poly(I·C) pretreatment (25 μg/ml) (see Materials and Methods). Poly(I·C) used under these conditions was shown to selectively engage TLR3 (38). To eliminate an influence of extracellular type I IFN, IFNAR-blocking antibody was added in combination with poly(I·C) (Fig. 7).

Treatment of DM440 cells with 25 μg/ml poly(I·C) (6 h) induced IFIT1 and p-STAT1 (Y701) in mock-infected cells (Fig. 7A). However, poly(I·C) treatment induced IFIT1 without an increase in p-STAT1 (Y701) in the presence of IFNAR2 blocking antibody, indicating that poly(I·C)-induced endogenous antiviral responses yielded an ISG signature, presumably via TLR3, in the absence of auto-/paracrine type I IFN signaling (Fig. 7A). PVSRIPO or EMCV infection (MOI of 0.1) did not change this pattern, except to produce a slight increase of IFIT1 and STAT1 induction, possibly attributable to the combined viral dsRNA/poly(I·C) stimulus (Fig. 7B and C). PVSRIPO translation did not change significantly in MDA5-depleted DM440 cells upon poly(I·C) treatment (Fig. 7B and D), confirming a theme of poliovirus innate antiviral subversion evident in all assays. In contrast, EMCV was profoundly inhibited by poly(I·C) treatment (Fig. 7C and D). Adding IFNAR-blocking antibody partially rescued EMCV translation in poly(I·C)-treated cells (Fig. 7C and D). We speculate that this reflects combined inhibitory effects of endogenous antiviral signatures (e.g., ISGs like IFIT1) and paracrine type I IFNs elicited by poly(I·C). IFNAR-blocking antibodies had no protective effect on EMCV translation in EMCV-infected (wild-type MDA5) DM440 cells because in that assay the only source of type I IFN was the infection itself (Fig. 5B and C). Thus, PVSRIPO subverts repression mediated by both TBK1/IKKε-activated IRF3 and paracrine type I IFN signaling in cancer cells.

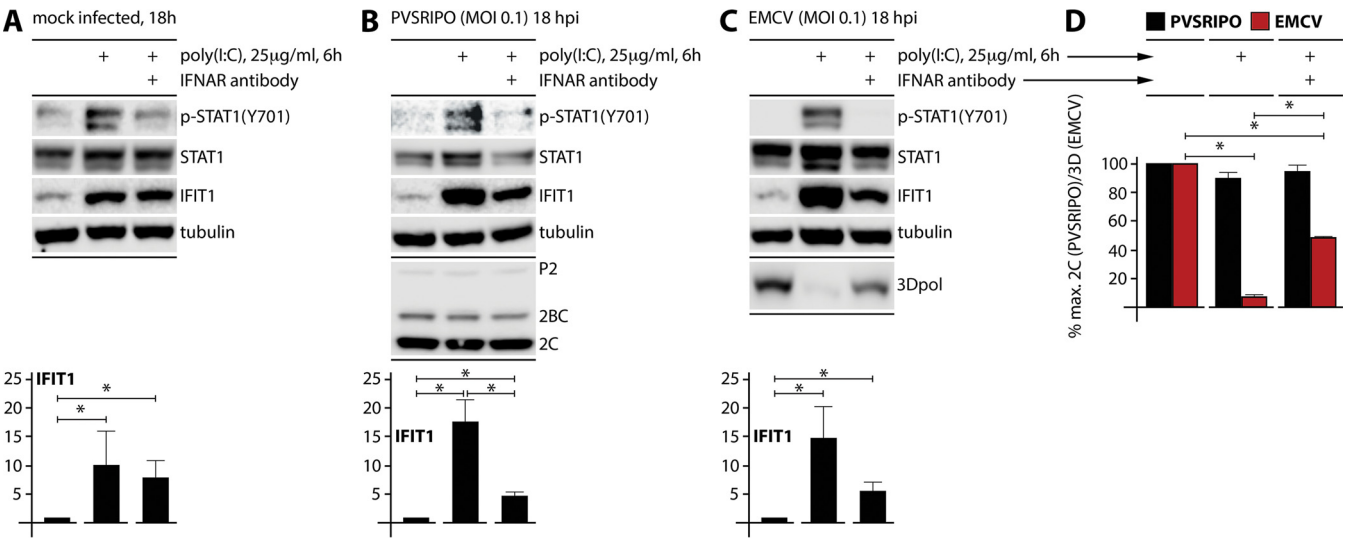

FIG 7 TLR3 activation in MDA5-depleted DM440 cells inhibits EMCV but not PVSRIPO. MDA5-depleted DM440 cells were pretreated with 1 μg/ml isotype-matched control antibody (mouse IgG2A) or IFNAR2 blocking monoclonal antibody (12 h), treated with 25 μg/ml extracellular poly(I·C) or vehicle (6 h), and then mock (0 h) or virus (MOI of 0.1; 18 h) infected. (A, B, and C) Lysates were collected from mock-, PVSRIPO-, and EMCV-infected DM440 cells and analyzed by immunoblotting for markers of viral translation (P2, 2BC, and 2C for PVSRIPO; $3D^{pol}$ for EMCV) and innate response [p-STAT1 (Y701), STAT1, and IFIT1]. Immunoblots are representative of two independent experiments. Bottom panels show the fold increase in IFIT1 after treatments (means ± SEM; $n = 2$). *, $P < 0.05$. (D) Viral protein expression in treated DM440 cells after PVSRIPO (2C) or EMCV ($3D^{pol}$) infection as a percentage of maximum detected viral protein (means ± SEM; $n = 2$). *, $P < 0.05$, for all $3D^{pol}$ differences. Differences in results for 2C were not statistically significant.

DISCUSSION

A central conundrum with harnessing recombinant viruses for oncolytic use is defining the relative contributions of viral cancer cell cytotoxicity versus proinflammatory activation (e.g., via innate antiviral responses) to therapy. This problem is particularly acute for PVSRIPO as diverse compartments in the tumor (notably neoplastic cells and tumor-associated myeloid cells) are infected with very different outcomes (12). PVSRIPO infection is associated with profuse release of inflammatory mediators from either compartment (12), with deep implications for cancer immunotherapy (39, 40).

In this study, we focused on the most elemental issue in this context: the PVSRIPO-host innate immune relation in infected cancer cells. We describe ongoing PVSRIPO translation and (resulting) cytotoxicity in the face of active innate antiviral immunity, even at extremely low MOIs where <0.001% of cells in a culture are infected initially. Deciphering the level of susceptibility with the IFN-sensitive picornavirus EMCV suggests vulnerability to endogenous events following PRR engagement, i.e., transcriptional programs in infected cells controlled by MAVS-enabled kinases. We believe that poliovirus's uniquely simple and efficacious life cycle, combined with drastic interference with host translation (in large part conveyed by $2A^{pro}$ activity, which EMCV lacks [41]), renders it relatively insensitive to these events.

Our studies conclude that PVSRIPO innate resistance occurs without any active interference with host innate antiviral activation. We cannot confirm the flurry of published reports suggesting that enteroviral proteases engage in targeted degradation of innate antiviral response modifiers. In all reported such instances, the extent of degradation was modest at best, invariably occurred in very late phases of the infection (when signs of enterovirus cytotoxicity abound), and were obtained with high MOIs of ≥10. To be relevant in the viral life cycle, substantial cleavage would have to occur very early, as is the case for the most rigorously defined and relevant host protein cleavages in enterovirus-infected cells, such as that of eIF4G1/2 (26). Moreover, we document IFN-β release, phosphorylation of STAT1 (Y701), and induction of ISGs with PVSRIPO infection of melanoma cells.

Our investigations raise the possibility of preclinical tests of PVSRIPO in immunocompetent rodent tumor models with targeted depletion of innate antiviral response

modifiers. We are not (yet) pursuing such studies for several reasons. First, depleting innate response mediators (e.g., IFNAR knockout) enhances tumor aggressiveness considerably. Second, depletion of specific innate response modifiers changes baseline expression of multiple nodes in the innate IFN response system, reducing the ability to interpret results. Third, and most importantly, the precise composition of the innate response to poliovirus (e.g., PVSRIPO) remains unknown and is subject to intense investigation in our laboratory.

Antiviral type I IFN responses, for their broad and potent costimulatory activation profile, are vital for successful cancer immunotherapy (42). Provoking type I IFN responses in infected tumor cells, without abrogating viral cytotoxicity and the presentation of endogenous tumor antigens against a backdrop of danger- and pathogen-associated molecular patterns (12, 40), may be particularly auspicious for PVSRIPO's capacity for instigating tumor-antigen-specific antitumor immunity.

MATERIALS AND METHODS

Cell lines and viruses. DM6, DM440, and DM443 melanoma cell lines were generous gifts from D. Tyler (University of Texas Medical Branch, Galveston, TX). DU54 glioma lines were described previously (9). All cell lines were maintained in Dulbecco's modified essential medium (DMEM) supplemented with 10% fetal bovine serum (FBS), 1× antibiotic-antimycotic, and nonessential amino acids (NEAA) (all Invitrogen). MDA5-depleted cell lines were grown in medium containing 1.5 μg/ml puromycin (Invitrogen). EMCV (ATCC VR-129B) and PVSRIPO were propagated in HeLa cells as previously described (9) and purified by filtration through a 0.45-μm-pore-size syringe filter followed by concentration through a 100-kDa filter (Millipore). Viral titers were measured by plaque assay in HeLa cells as described previously (2).

Generation of MDA5 knockdown cell lines. Lentiviral shRNA transduction vectors were produced from Mission shRNA plasmid DNA with the shRNA sequence 5′-CCGGCCCATGACACAGAATGAACAACTC GAGTTGTTCATTCTGTGTCATGGGTTTTTG (Sigma-Aldrich) using ViraPower lentiviral packaging mix in 293FT cells (Invitrogen) according to the manufacturer's instructions. Stable MDA5 knockdown DM440 and DM6 cells were generated by lentiviral transduction in DMEM containing 8 μg/ml Polybrene (Millipore), followed by selection with growth medium containing 1.5 μg/ml puromycin (Invitrogen), colony picking, and expansion. Candidate knockdown clones were screened by transfection with Lipofectamine 2000 (Thermo Fisher) and 10 μg/ml high-molecular-weight poly(I·C) (Invivogen) or Lipofectamine 2000 alone (24 h), followed by assessment of MDA5 loss.

Viral infections and multistep growth curves. Melanoma cells were plated at 80 to 90% confluence after 24 h of incubation in growth medium at 37°C in 5% CO_2. Cells from two randomly selected dishes from each experiment were trypsinized, stained with trypan blue, and counted with a Countess II automated cell counter (Invitrogen) per the manufacturer's protocol. DM440, DM443, and DM6 cells were infected at the indicated MOI (see legends to Fig. 1 to 7) by removing medium and replacing it with 1 ml of prewarmed growth medium containing virus or medium alone (mock infection) and incubated at 37°C in 5% CO_2. For multistep growth curves, cells were incubated with virus-containing medium (1 h) at 37°C in 5% CO_2 and washed once with phosphate-buffered saline (PBS), and 1 ml of prewarmed virus free growth medium was added to cells. Cells were incubated at 37°C in 5% CO_2 for the indicated time (see legends to Fig. 1 to 7) and then subjected to two freeze-thaw cycles. Viral titers were determined by plaque assay, as described previously (12), and the numbers of PFU/cell were calculated based on cell number at 0 hpi.

Treatment with IFN, IFNAR blocking, TLR3 activation, and TBK1/IKKε inhibition. Four hundred thousand cells were plated in 35-mm tissue culture dishes. Following 24 h of incubation at 37°C in 5% CO_2, the growth medium was removed and replaced with 1 ml of growth medium containing 100 U/ml recombinant human IFN-α2a (PBL Assay Science) and incubated for 24 h at 37°C in 5% CO_2 and then infected as described above (17). For blocking IFNAR, either 2×10^4 or 4×10^5 cells were plated in 24-well tissue culture dishes in 0.5 ml of growth medium or in six-well tissue culture dishes in 1 ml of growth medium, respectively, containing 1 μg/ml mouse anti-human IFNAR2 antibody (clone MMHAR-2; PBL Assay Science), 1 μg/ml mouse IgG2A (R&D Systems) isotype control, or no antibody (43). Following overnight incubation at 37°C and 5% CO_2, cells were infected as described above with prewarmed growth medium containing virus plus the previous antibody treatment. Alternatively, following antibody pretreatment, 25 μg/ml poly(I·C) (Sigma-Aldrich) was added to cells (6 h), where indicated (see legend to Fig. 7), and cells were treated with growth medium containing virus and 1 μg/ml antibody, as described above. For TBK1/IKKε inhibition, 8×10^5 cells were plated in 35-mm tissue culture dishes and incubated at 37°C in 5% CO_2 (24 h). The growth medium was replaced with 1 ml of prewarmed growth medium containing 10 μM BX795 (Invivogen) or an equal volume of dimethyl sulfoxide (DMSO) prior to infection.

Cell lysis and immunoblot assays. Cells were lysed at the indicated time points (see legends to Fig. 1 to 7) as described previously (44) in polysomal lysis buffer (PLB) (20 mM Tris, pH 7.4, 100 mM NaCl, 5 mM $MgCl_2$, 0.5% Igepal CA-630, NP-40 [Sigma], 1× Halt protease and phosphatase inhibitor cocktail [Thermo Scientific]). Samples were prepared for SDS-PAGE by addition of 4× lithium dodecyl sulfate (LDS) buffer containing 20% β-mercaptoethanol (Sigma-Aldrich). All LDS-containing samples were subjected to SDS-PAGE and Western blotting as described previously (12) using antibodies against

eIF4G1, p-STAT1 (Y701), STAT1, PARP, glyceraldehyde-3-phosphate dehydrogenase (GAPDH), OAS1, eIF4A, IFIT1 (Cell Signaling Technologies), MDA5 (Enzo Life Sciences), cardiovirus $3D^{Pol}$ (Santa Cruz Biotechnology), poliovirus 2C, and tubulin (Sigma-Aldrich). MAVS antibody was a generous gift from Stacy Horner (Duke University). An Odyssey Fc imager (Li-Cor Biosciences) was used to image and quantify immunoblots. Protein quantification was calculated with Li-Cor Image Studio software and expressed relative to the level of the loading control. Cellular protein levels were standardized to expression in mock-treated controls and are depicted as the fold increase above the mock treatment level while viral protein expression was standardized relative to the maximum detected viral protein in each interval.

IFN-β ELISA and LDH release assay. Medium was collected from cells at the indicated time points (see legends to Fig. 1 and 3) and centrifuged at 500 $\times$ *g* (5 min), and supernatant was frozen at -80°C. An IFN-β enzyme-linked immunosorbent assay (ELISA) was performed on supernatants from infected and mock-infected cells in parallel and in duplicate from at least four independent experiments with a VeriKine-HS human interferon beta serum ELISA kit (PBL Biosciences) according to the manufacturer's protocol. An LDH release assay was performed with an LDH cytotoxicity kit (Thermo Fisher) as described by Brown et al. (12), per the manufacturer's protocol, using supernatant from freeze-thawed cells as a 100% cell lysis control and supernatant from mock-infected cells at 0 hpi as a 0% lysis control.

Statistical analyses. All data are shown as means $\pm$ standard errors of means (SEM). Statistical significance was determined by one- or two-way analysis of variance (ANOVA), followed by appropriate *post hoc* Tukey's or Sidak's multiple-comparison test; *P* values of <0.05 were considered statistically significant.

ACKNOWLEDGMENTS

This work was supported by Public Health Service awards R01-CA124756 (M.G.) and F32-CA22493 (M.C.B.). In addition, we acknowledge support by the Levkowsky Family Foundation and the BLAST Glioblastoma Foundation.

REFERENCES

1. Desjardins A, Gromeier M, Herndon JE, II, Beaubier N, Bolognesi DP, Friedman AH, Friedman HS, McSherry F, Muscat AM, Nair S, Peters KB, Randazzo D, Sampson JH, Vlahovic G, Harrison WT, McLendon RE, Ashley D, Bigner DD. 12 July 2018. Recurrent glioblastoma treated with recombinant poliovirus. N Engl J Med https://doi.org/10.1056/NEJMoa1716435.
2. Gromeier M, Alexander L, Wimmer E. 1996. Internal ribosomal entry site substitution eliminates neurovirulence in intergeneric poliovirus recombinants. Proc Natl Acad Sci U S A 93:2370–2375.
3. Gromeier M, Lachmann S, Rosenfeld MR, Gutin PH, Wimmer E. 2000. Intergeneric poliovirus recombinants for the treatment of malignant glioma. Proc Natl Acad Sci U S A 97:6803–6808. https://doi.org/10.1073/pnas.97.12.6803.
4. Merrill MK, Dobrikova EY, Gromeier M. 2006. Cell-type-specific repression of internal ribosome entry site activity by double-stranded RNA-binding protein 76. J Virol 80:3147–3156. https://doi.org/10.1128/JVI.80.7.3147-3156.2006.
5. Merrill MK, Gromeier M. 2006. The double-stranded RNA binding protein 76:NF45 heterodimer inhibits translation initiation at the rhinovirus type 2 internal ribosome entry site. J Virol 80:6936–6942. https://doi.org/10.1128/JVI.00243-06.
6. Chandramohan V, Bryant JD, Piao H, Keir ST, Lipp ES, Lefaivre M, Perkinson K, Bigner DD, Gromeier M, McLendon RE. 2017. Validation of an immunohistochemistry assay for detection of CD155, the poliovirus receptor, in malignant gliomas. Arch Pathol Lab Med 141:1697–1704. https://doi.org/10.5858/arpa.2016-0580-OA.
7. Takai Y, Miyoshi J, Ikeda W, Ogita H. 2008. Nectins and nectin-like molecules: roles in contact inhibition of cell movement and proliferation. Nat Rev Mol Cell Biol 9:603–615. https://doi.org/10.1038/nrm2457.
8. Dobrikova EY, Goetz C, Walters RW, Lawson SK, Peggins JO, Muszynski K, Ruppel S, Poole K, Giardina SL, Vela EM, Estep JE, Gromeier M. 2012. Attenuation of neurovirulence, biodistribution, and shedding of a poliovirus:rhinovirus chimera after intrathalamic inoculation in Macaca fascicularis. J Virol 86:2750–2759. https://doi.org/10.1128/JVI.06427-11.
9. Brown MC, Bryant JD, Dobrikova EY, Shveygert M, Bradrick SS, Chandramohan V, Bigner DD, Gromeier M. 2014. Induction of viral, 7-methylguanosine cap-independent translation and oncolysis by mitogen-activated protein kinase-interacting kinase-mediated effects on the serine/arginine-rich protein kinase. J Virol 88:13135–13148. https://doi.org/10.1128/JVI.01883-14.
10. Brown MC, Dobrikov MI, Gromeier M. 2014. Mitogen-activated protein kinase-interacting kinase regulates mTOR/AKT signaling and controls serine/arginine-rich protein kinase-responsive type 1 internal ribosome entry site-mediated translation and viral oncolysis. J Virol 88:13149–13160. https://doi.org/10.1128/JVI.01884-14.
11. Brown MC, Gromeier M. 2017. MNK controls mTORC1:substrate association through regulation of TELO2 binding with mTORC1. Cell Rep 18:1444–1457. https://doi.org/10.1016/j.celrep.2017.01.023.
12. Brown MC, Holl EK, Boczkowski D, Dobrikova E, Mosaheb M, Chandramohan V, Bigner DD, Gromeier M, Nair SK. 2017. Cancer immunotherapy with recombinant poliovirus induces IFN-dominant activation of dendritic cells and tumor antigen-specific CTLs. Sci Transl Med 9:eaan4220. https://doi.org/10.1126/scitranslmed.aan4220.
13. Ruotsalainen JJ, Kaikkonen MU, Niittykoski M, Martikainen MW, Lemay CG, Cox J, De Silva NS, Kus A, Falls TJ, Diallo J-S, Le Boeuf F, Bell JC, Ylä-Herttuala S, Hinkkanen AE, Vähä-Koskela MJ. 2015. Clonal variation in interferon response determines the outcome of oncolytic virotherapy in mouse CT26 colon carcinoma model. Gene Ther 22:65–75. https://doi.org/10.1038/gt.2014.83.
14. Jackson JD, Markert JM, Li L, Carroll SL, Cassady KA. 2016. STAT1 and NF-κB inhibitors diminish basal interferon-stimulated gene expression and improve the productive infection of oncolytic HSV in MPNST cells. Mol Cancer Res 14:482–492. https://doi.org/10.1158/1541-7786.MCR-15-0427.
15. Westcott MM, Liu J, Rajani K, D'Agostino R, Lyles DS, Porosnicu M. 2015. Interferon beta and interferon alpha 2a differentially protect head and neck cancer cells from vesicular stomatitis virus-induced oncolysis. J Virol 89:7944–7954. https://doi.org/10.1128/JVI.00757-15.
16. Berchtold S, Lampe J, Weiland T, Smirnow I, Schleicher S, Handgretinger R, Kopp H-G, Reiser J, Stubenrauch F, Mayer N, Malek NP, Bitzer M, Lauer UM. 2013. Innate immune defense defines susceptibility of sarcoma cells to measles vaccine virus-based oncolysis. J Virol 87:3484–3501. https://doi.org/10.1128/JVI.02106-12.
17. Morrison JM, Racaniello VR. 2009. Proteinase $2A^{pro}$ is essential for enterovirus replication in type I interferon-treated cells. J Virol 83:4412–4422. https://doi.org/10.1128/JVI.02177-08.
18. Feng Q, Hato SV, Langereis MA, Zoll J, Virgen-Slane R, Peisley A, Hur S, Semler BL, van Rij RP, van Kuppeveld FJ. 2012. MDA5 detects the double-stranded RNA replicative form in picornavirus-infected cells. Cell Rep 2:1187–1196. https://doi.org/10.1016/j.celrep.2012.10.005.
19. Kato H, Takeuchi O, Sato S, Yoneyama M, Yamamoto M, Matsui K, Uematsu S, Jung A, Kawai T, Ishii KJ, Yamaguchi O, Otsu K, Tsujimura T,

Koh CS, Reis e Sousa C, Matsuura Y, Fujita T, Akira S. 2006. Differential roles of MDA5 and RIG-I helicases in the recognition of RNA viruses. Nature 441:101–105. https://doi.org/10.1038/nature04734.
20. Fitzgerald KA, McWhirter SM, Faia KL, Rowe DC, Latz E, Golenbock DT, Coyle AJ, Liao SM, Maniatis T. 2003. IKKepsilon and TBK1 are essential components of the IRF3 signaling pathway. Nat Immunol 4:491–496. https://doi.org/10.1038/ni921.
21. Loo YM, Gale M, Jr. 2011. Immune signaling by RIG-I-like receptors. Immunity 34:680–692. https://doi.org/10.1016/j.immuni.2011.05.003.
22. Schoggins JW, Rice CM. 2011. Interferon-stimulated genes and their antiviral effector functions. Curr Opin Virol 1:519–525. https://doi.org/10.1016/j.coviro.2011.10.008.
23. Casado JG, Pawelec G, Morgado S, Sanchez-Correa B, Delgado E, Gayoso I, Duran E, Solana R, Tarazona R. 2009. Expression of adhesion molecules and ligands for activating and costimulatory receptors involved in cell-mediated cytotoxicity in a large panel of human melanoma cell lines. Cancer Immunol Immunother 58:1517–1526. https://doi.org/10.1007/s00262-009-0682-y.
24. Li XY, Das I, Lepletier A, Addala V, Bald T, Stannard K, Barkauskas D, Liu J, Aguilera AR, Takeda K, Braun M, Nakamura K, Jacquelin S, Lane SW, Teng MW, Dougall WC, Smyth MJ. 2018. CD155 loss enhances tumor suppression via combined host and tumor-intrinsic mechanisms. J Clin Invest 128:2613–2625. https://doi.org/10.1172/JCI98769.
25. Davies H, Bignell GR, Cox C, Stephens P, Edkins S, Clegg S, Teague J, Woffendin H, Garnett MJ, Bottomley W, Davis N, Dicks E, Ewing R, Floyd Y, Gray K, Hall S, Hawes R, Hughes J, Kosmidou V, Menzies A, Mould C, Parker A, Stevens C, Watt S, Hooper S, Wilson R, Jayatilake H, Gusterson BA, Cooper C, Shipley J, Hargrave D, Pritchard-Jones K, Maitland N, Chenevix-Trench G, Riggins GJ, Bigner DD, Palmieri G, Cossu A, Flanagan A, Nicholson A, Ho JW, Leung SY, Yuen ST, Weber BL, Seigler HF, Darrow TL, Paterson H, Marais R, Marshall CJ, Wooster R, et al. 2002. Mutations of the BRAF gene in human cancer. Nature 417:949–954. https://doi.org/10.1038/nature00766.
26. Etchison D, Milburn SC, Edery I, Sonenberg N, Hershey JW. 1982. Inhibition of HeLa cell protein synthesis following poliovirus infection correlates with the proteolysis of a 220,000-dalton polypeptide associated with eucaryotic initiation factor 3 and a cap binding protein complex. J Biol Chem 257:14806–14810.
27. Strauss M, Filman DJ, Belnap DM, Cheng N, Noel RT, Hogle JM. 2015. Nectin-like interactions between poliovirus and its receptor trigger conformational changes associated with cell entry. J Virol 89:4143–4157. https://doi.org/10.1128/JVI.03101-14.
28. Fenwick ML, Cooper PD. 1962. Early interactions between poliovirus and ERK cells: some observations on the nature and significance of the rejected particles. Virology 18:212–223. https://doi.org/10.1016/0042-6822(62)90007-7.
29. Katze MG, He Y, Gale M, Jr. 2002. Viruses and interferon: a fight for supremacy. Nat Rev Immunol 2:675–687. https://doi.org/10.1038/nri888.
30. Feng Q, Langereis MA, Lork M, Nguyen M, Hato SV, Lanke K, Emdad L, Bhoopathi P, Fisher PB, Lloyd RE, van Kuppeveld FJ. 2014. Enteroviruses $2A^{pro}$ targets MDA5 and MAVS in infected cells. J Virol 88:3369–3378. https://doi.org/10.1128/JVI.02712-13.
31. Barral PM, Morrison JM, Drahos J, Gupta P, Sarkar D, Fisher PB, Racaniello VR. 2007. MDA-5 is cleaved in poliovirus-infected cells. J Virol 81:3677–3684. https://doi.org/10.1128/JVI.01360-06.
32. Mukherjee A, Morosky SA, Delorme-Axford E, Dybdahl-Sissoko N, Oberste MS, Wang T, Coyne CB. 2011. The coxsackievirus B 3C protease cleaves MAVS and TRIF to attenuate host type I interferon and apoptotic signaling. PLoS Pathog 7:e1001311. https://doi.org/10.1371/journal.ppat.1001311.
33. Gromeier M, Wetz K. 1990. Kinetics of poliovirus uncoating in HeLa cells in a nonacidic environment. J Virol 64:3590–3597.
34. Shuai K, Ziemiecki A, Wilks AF, Harpur AG, Sadowski HB, Gilman MZ, Darnell JE. 1993. Polypeptide signalling to the nucleus through tyrosine phosphorylation of Jak and Stat proteins. Nature 366:580–583. https://doi.org/10.1038/366580a0.
35. Meraz MA, White JM, Sheehan KC, Bach EA, Rodig SJ, Dighe AS, Kaplan DH, Riley JK, Greenlund AC, Campbell D, Carver-Moore K, DuBois RN, Clark R, Aguet M, Schreiber RD. 1996. Targeted disruption of the Stat1 gene in mice reveals unexpected physiologic specificity in the JAK-STAT signaling pathway. Cell 84:431–442. https://doi.org/10.1016/S0092-8674(00)81288-X.
36. Yao H, Dittmann M, Peisley A, Hoffmann HH, Gilmore RH, Schmidt T, Schmidt-Burgk J, Hornung V, Rice CM, Hur S. 2015. ATP-dependent effector-like functions of RIG-I-like receptors. Mol Cell 58:541–548. https://doi.org/10.1016/j.molcel.2015.03.014.
37. Clark K, Plater L, Peggie M, Cohen P. 2009. Use of the pharmacological inhibitor BX795 to study the regulation and physiological roles of TBK1 and IkappaB kinase epsilon: a distinct upstream kinase mediates Ser-172 phosphorylation and activation. J Biol Chem 284:14136–14146. https://doi.org/10.1074/jbc.M109.000414.
38. Alexopoulou L, Holt AC, Medzhitov R, Flavell RA. 2001. Recognition of double-stranded RNA and activation of NF-κB by Toll-like receptor 3. Nature 413:732–738. https://doi.org/10.1038/35099560.
39. Brown MC, Gromeier M. 2015. Oncolytic immunotherapy through tumor-specific translation and cytotoxicity of poliovirus. Discov Med 19:359–365.
40. Brown MC, Gromeier M. 2015. Cytotoxic and immunogenic mechanisms of recombinant oncolytic poliovirus. Curr Opin Virol 13:81–85. https://doi.org/10.1016/j.coviro.2015.05.007.
41. Jen G, Detjen BM, Thach RE. 1980. Shutoff of HeLa cell protein synthesis by encephalomyocarditis virus and poliovirus: a comparative study. J Virol 35:150–156.
42. Zitvogel L, Galluzzi L, Kepp O, Smyth MJ, Kroemer G. 2015. Type I interferons in anticancer immunity. Nat Rev Immunol 15:405–414. https://doi.org/10.1038/nri3845.
43. Tsugawa Y, Kato H, Fujita T, Shimotohno K, Hijikata M. 2014. Critical role of interferon-alpha constitutively produced in human hepatocytes in response to RNA virus infection. PLoS One 9:e89869. https://doi.org/10.1371/journal.pone.0089869.
44. Dobrikov M, Dobrikova E, Shveygert M, Gromeier M. 2011. Phosphorylation of eukaryotic translation initiation factor 4G1 (eIF4G1) by protein kinase Cα regulates eIF4G1 binding to Mnk1. Mol Cell Biol 31:2947–2959. https://doi.org/10.1128/MCB.05589-11.